EPSC Abstracts
Vol. 19, EPSC2026-533, 2026, updated on 18 Nov 2026
https://doi.org/10.5194/epsc2026-533
Europlanet Science Congress 2026
© Author(s) 2026. This work is distributed under
the Creative Commons Attribution 4.0 License.

Beyond Constriction Resistance: Multicomponent Microscale Conduction Model

Bhuvan Agrawal[1], Moritz Goldmann[2], Matthias Grott[1], Jürgen Blum[3], Jens Biele[4], Carsten Güttler[2], Bastian Gundlach[2], Jörg Kollenberg[1], Markus Patzek[2], and Ansgar Greshake[5]

[1]German Aerospace Center, Berlin, Germany
[2]Universität Münster, Münster, Germany
[3]Technische Universität Braunschweig, Braunschweig, Germany
[4]German Aerospace Center, Cologne, Germany
[5]Museum für Naturkunde, Berlin, Germany

Introduction. Accurate thermophysical modeling of asteroid boulders is crucial for interpreting thermal data from planetary missions such as Hayabusa2 and OSIRIS-REx [1, 2]. Interpreting these measurements require understanding the evolutionary processes of asteroid materials, such as mechanical settling, hot and cold pressing, and natural sintering during their formation [3, 4]. Numerical simulations based on discrete element method (DEM) are among primary tools for evaluating heat transfer in these granular and porous systems. However, standard DEM frameworks typically collapse contact physics into a single effective conductance parameter. In particular, classical models widely assume normalized contact radius (r_c/r_p), where r_c and r_p are the radius of contact and particle respectively, to be the sole parameter controlling contact resistance [5, 6]. Consequently, current formulations rely heavily on empirical calibration against macroscopic bulk thermal conductivity measurements [7-10]. This empirical tuning restricts the applicability of current models when extrapolating to a variable-contact environments with microstructural realities of asteroid boulders. There is a need to assess additional contact-scale resistance pathways and their effect on aggregate-scale conductivity to bridge the gap between numerical simulations and physical reality.

Comparative Framework. To model solid-phase heat transfer, conventional thermal DEM implementations fundamentally rely on classical constriction resistance, which occurs because heat flow lines must bend and squeeze through the point contacts [11, 12]. These models, however, frequently omit broader micro-scale transport phenomena that become critical at larger contact areas. In this comparative study, we expand upon this standard baseline by explicitly incorporating three additional thermal resistance mechanisms: a constriction alleviation factor to correct for large contact radius ratios [13, 14], internal particle resistance associated with finite thermal pathways within the particles [15], and grain-boundary thermal resistance [16]. As shown in Figure 1, the relative importance of these mechanisms varies strongly with particle radius and material microstructure.

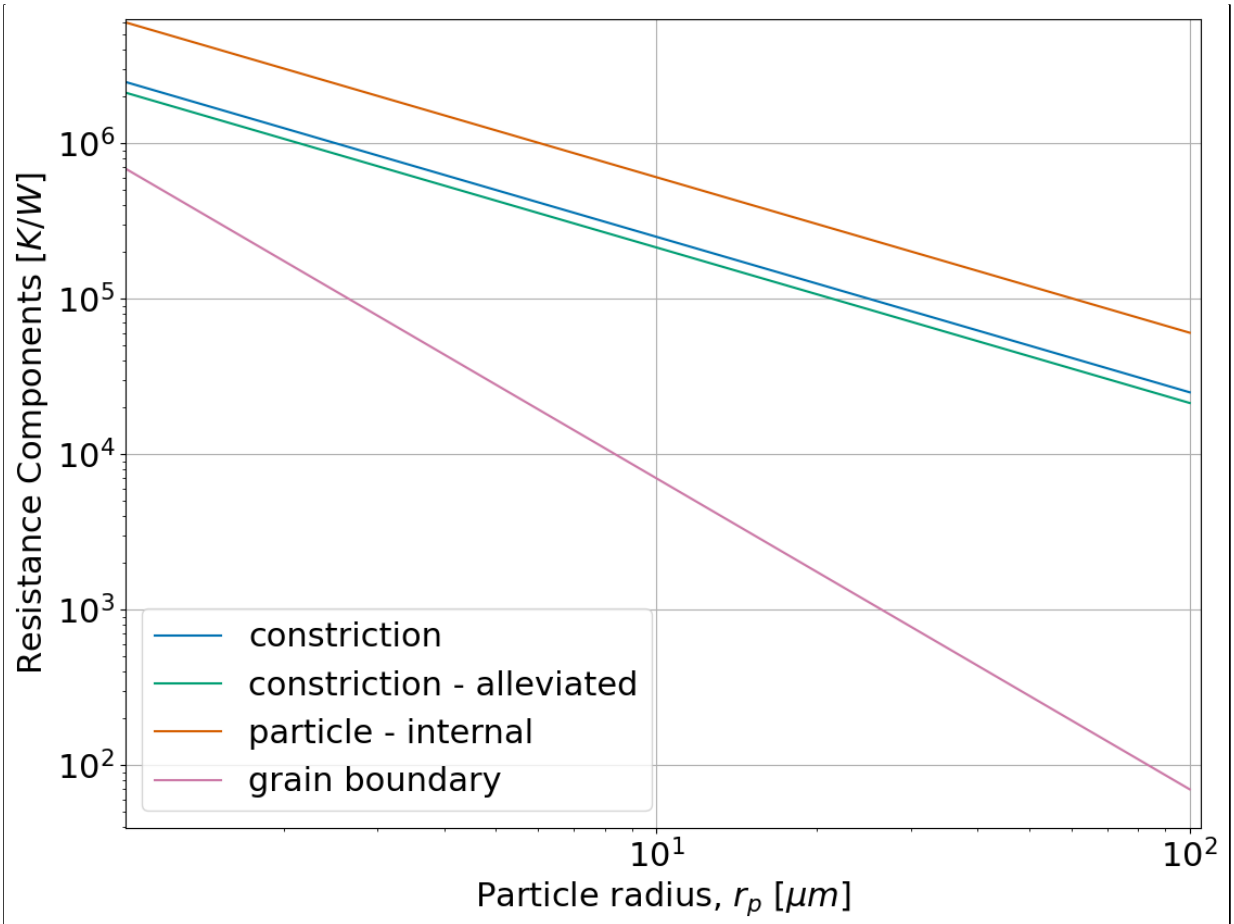

Figure 1. Resistance contributions at particle-particle contact as a function of particle radius. For this calculation, a 10% contact radius was assumed with a diametric heat path within the particle.

Method. To scale this contact-level thermal physics to macroscopic observables, we modified the open-source DEM code LIGGGHTS [17] to explicitly evaluate the four heat transfer mechanisms at every particle-particle contact. Porous aggregates are represented as assemblies of uniformly sized spheres. To systematically isolate the effects of each heat transfer mode, we designed a series of independent simulations where different subsets of the thermal mechanisms are activated. The bulk thermal conductivity of the particle assembly is then calculated at macroscopic thermal equilibrium, alongside coordination number and porosity, as detailed in [18].

Results. The relative contributions of the different thermal resistance terms were examined as a function of normalized contact radius (Figure 2). The preliminary contact-scale analysis indicates particle resistance, associated with finite thermal pathways within the particles, can become a major contribution to the total thermal resistance and tends to increase with growing contact radius. In contrast, grain-boundary resistance remains comparatively small and decreases as the normalized contact radius increases. The inclusion of constriction alleviation factor also modifies the response of the baseline constriction resistance. It causes a reduction in associated resistance as the normalized contact radius increased. These contact-scale results suggest that heat transfer cannot always be described by constriction resistance or normalized contact radius alone.

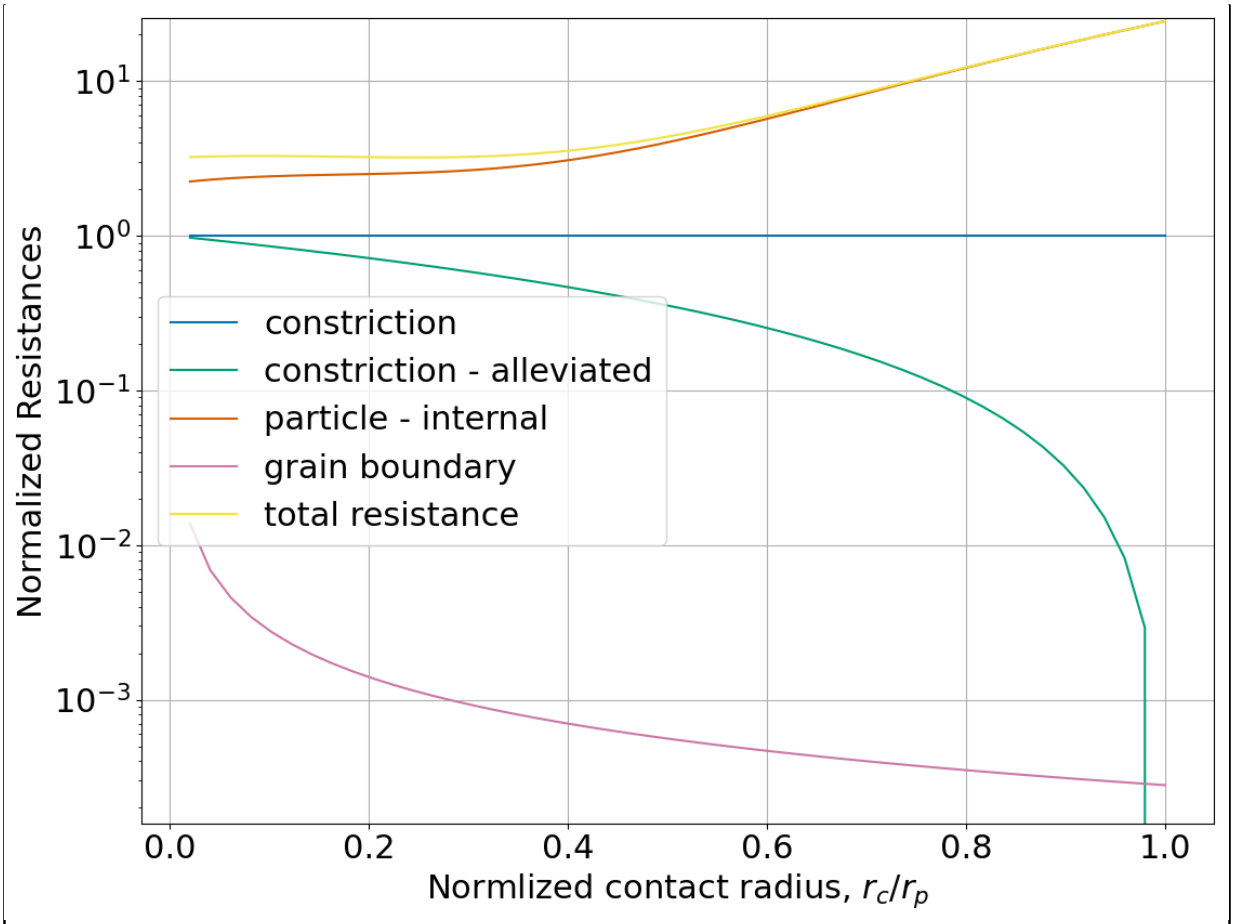

Figure 2. Resistance contributions to particle-particle contacts normalized by classical constriction resistance with respect to normalized contact radius. The intrinsic particle conductivity is assumed to be unity with diametric heat path ways within the particles.

Outlook. These contact-scale findings provide the basis for the next stage of the study, in which their influences on macroscopic bulk thermal conductivity will be examined using thermal DEM simulations. The modified model will first be benchmarked using idealized regular packings and then applied to randomly packed assemblies. Finally, the resulting bulk thermal conductivities calculated using these random packings will be compared with laboratory experiments conducted on glass beads [19]. This step-by-step upscaling is intended to clarify which contact-scale mechanisms remain relevant at assembly scale, ultimately improving our understanding of the relationship between microscopic grain interactions and the macroscopic thermophysical properties of highly porous asteroid boulders.

References

1. Okada et al., Space Sci Rev 2017, 208, 255-286.
2. Lauretta et al., Space Sci Rev 2017, 212, 925-984.
3. Grott et al., Nature Astronomy 2019, 3, 971-976.
4. Hamm et al., MNRAS 2020, 496, 2776-2785.
5. Batchelor and O'Brien, Proc. A 1977, 355, 313-333.
6. Zhu and Li, Int. J. Heat Mass Transfer 2021, 167, 120723.
7. Sakatani et al., AIP Advances 2017, 7, 015310.
8. Arakawa et al., Icarus 2019, 324, 8-14.
9. Gundlach and Blum, Icarus 2013, 223, 479-492.

10. Henke et al., A&A 2016, 589, A41.
11. Madhusudana, Thermal Contact Conductance, Springer Cham, 2nd Edition, 2014
12. Chaudhuri et al., Chemical Engineering Science 2006, 61, 6348-6360.
13. Cooper et al., Int. J. Heat Transfer 1969, 12, 279-300.
14. Mikic, Int. J. Heat Transfer 1974, 17, 205-214.
15. Siu and Lee, Int. J. Heat Mass Transfer 2000, 43, 3917-3924.
16. Smith et al., J. Am. Ceram. Soc. 2003, 86, 105-111.
17. Kloss et al., Progress in Computational Fluid Dynamics 2012, 12, 140-152.
18. Agrawal et al, PSJ 2026, Submitted.
19. Goldmann et al, EPSC 2026 Abstract.